Published in IET Microwaves, Antennas & Propagation
Received on 15th April 2009
Revised on 17th October 2009
doi: 10.1049/iet-map.2009.0147

In Special Issue on Selected Papers from Mosharaka International Conference on Communications, Propagation and Electronics (MIC-CPE 2009)

ISSN 1751-8725

Antenna benchmark performance and array synthesis using central force optimisation

G.M. Qubati[1] *R.A. Formato*[2] *N.I. Dib*[1]

[1]*Electrical Engineering Department, Jordan University of Science & Technology, P.O. Box 3030, Irbid 22110, Jordan*
[2]*Registered Patent Attorney & Consulting Engineer, P.O. Box 1714, Harwich, MA 02645, USA*
E-mail: nihad@just.edu.jo

Abstract: Central force optimisation (CFO) is a new deterministic multi-dimensional search evolutionary algorithm (EA) inspired by gravitational kinematics. CFO is a simple technique that is still in its infancy. This study evaluates CFO's performance and provides further examples of its effectiveness by applying it to a set of 'real-world' antenna benchmarks and to pattern synthesis for linear and circular array antennas. A new selection scheme is introduced that enhances CFO's global search ability while maintaining its simplicity. The improved CFO algorithm is applied to the design of a circular array with very good results. CFO's performance on the antenna benchmarks and the synthesis problems is compared to that of other EAs.

1 Introduction

Central force optimisation (CFO) is an optimisation algorithm analogising gravitational kinematics [1, 2]. Many nature inspired metaheuristics are based on biological metaphors, for example, particle swarm optimisation (PSO) [3] (swarming behaviour of bees, fish and birds), or ant colony optimisation (ACO) [4] (foraging behaviour of ants). These EAs are inherently stochastic, unlike CFO which is deterministic.

This paper applies CFO to the design of a set of 'real-world' antenna benchmarks (proposed in [5]) and to the design of linear and circular antenna arrays. To enhance its global search ability while keeping its simplicity, a new selection scheme also is introduced in this paper, which then is applied to the design of a circular antenna array. This paper is divided as follows: Section 2 briefly describes the CFO algorithm. Section 3 presents the CFO results for the antenna benchmarks compared to those obtained using other optimisation techniques. Section 4 applies CFO to the design of a linear antenna array. In Section 5, a new selection scheme is introduced which then is applied to the design of a circular array in Section 6.

2 CFO algorithm

CFO locates the maxima of an objective function $f(x_i, \ldots, x_{N_d})$ by 'flying' a set of 'probes' through the decision space (DS) along trajectories computed using the gravitational analogy. In an N_d-dimensional real-valued decision space (DS), each 'probe' p ('particle' in PSO terminology) with position vector $\boldsymbol{R}_{j-1}^{p} \in \mathbb{R}^{N_d}$ experiences an acceleration $\boldsymbol{A}_{j-1}^{p}$ at the discrete time step $(j-1)$ given by [1]

$$\boldsymbol{A}_{j-1}^{p} = G \sum_{\substack{k=1 \\ k \neq p}}^{N_p} U(M_{j-1}^{k} - M_{j-1}^{p})(M_{j-1}^{k} - M_{j-1}^{p})^{\alpha} \times \frac{(\boldsymbol{R}_{j-1}^{k} - \boldsymbol{R}_{j-1}^{p})}{\|\boldsymbol{R}_{j-1}^{k} - \boldsymbol{R}_{j-1}^{p}\|^{\beta}} \quad (1)$$

where N_p is the total number of probes; $p = 1, \ldots, N_p$, the probe number; $j = 0, \ldots, N_t$ the time step; G the 'gravitational constant'; $\boldsymbol{A}_{j-1}^{p}$ the acceleration of probe p at step $j-1$; $\boldsymbol{R}_{j-1}^{p}$ the position vector of p at step $j-1$; $M_{j-1}^{p} = f(\boldsymbol{R}_{j-1}^{p})$ the fitness at probe p at step $j-1$; $U(\,)$ the unit step; and β, α the 'CFO exponents.'

CFO 'mass' is defined as the difference of fitnesses raised to the power α multiplied by the unit step; it is not the value of the objective function. The user defines mass in CFO space, and other functions could be used instead. But including the unit step $U(\,)$ is an essential element because it creates positive mass thereby insuring that CFO's 'gravity' is attractive. Each probe's position vector at step j is

updated according to the second equation of motion

$$\boldsymbol{R}_j^p = \boldsymbol{R}_{j-1}^p + \frac{1}{2}\boldsymbol{A}_{j-1}^p \Delta t^2, \quad j \geq 1 \tag{2}$$

Δt in (2) is the time step increment (unity in this paper). CFO starts with user-specified initial probe position and acceleration distributions, which may be deterministic or random. The initial acceleration vectors are zero in this paper.

Probes may fly outside the DS, and should be returned if they do. There are many possible probe retrieval methods. A useful one is the reposition factor F_{rep}, which can play an important role in CFO's convergence [2, 6]. It is shown schematically in Fig. 1.

F_{rep} is usually set to 0.5 or 0.9, or it may be variable. $R_k^{\min}$ and $R_k^{\max}$ are the minimum and maximum values of the kth spatial dimension corresponding to the optimisation problem constraints, or they are chosen to define the DS so as to include expected global optima.

Because CFO is inherently deterministic, it provides reproducibility and control over computed results. However, in this paper, local trapping is mitigated by adding a stochastic component. Algorithms that are inherently stochastic, PSO or ACO, for example, fail if randomness is removed. But, if randomness is added to CFO, it does not fail. The hybrid deterministic–stochastic approach is adopted for the array synthesis problems with very good results, while the benchmark ('BM') problems are treated deterministically. The CFO algorithm flowchart appears in Fig. 2.

3 CFO performance on the PBM antenna benchmarks

This section describes CFO's performance on the 'real-world' antenna benchmarks developed in [5] ('PBM', the 5-problem antenna benchmark suite, developed by Pantoja, Bretones and Martin). Two performance measures are used to evaluate how good an evolutionary algorithm (EA) is: effectiveness (accurately locating maxima) and efficiency (minimum computational effort). Algorithms that do not locate global maxima are ineffective; and any algorithm's utility is inversely proportional to how many calculations it requires. These measures are used to compare CFO to the four EAs in [5].

3.1 Overview of the PBM problems

There are five problems in the PBM suite whose properties appear in Table 1. N_{d} is the problem dimensionality, while x_1 and x_2, respectively, are the abscissa and ordinate in the two-dimensional (2D) DSs. For BM #5, the d_i are the array's centre-to-centre element spacing. λ is the wavelength. In each case the optimisation objective is to maximise the antenna's directivity. The first four problems are 2D, where the last one is $(N_{\text{el}}-1)$D, where N_{el} is the number of array elements. Antenna details, and the nature and complexity of the 2D DSs' topologies ('landscapes'), are described in [5]. Unimodal BM #1 and BM #4 have one global maximum, but the first landscape is 'lumpy' with strong local maxima, whereas the second one is 'smooth.' BM #2 adds noise to an already complex topology with large amplitude local maxima close to a single global maximum. BM #3 is extremely multimodal with four global maxima. BM #5 is unimodal with a dimensionality determined by the number of elements in a collinear dipole array.

3.2 NEC4 validation

The PBM suite in [5] was solved numerically using NEC (numerical electromagnetics code). To validate CFO's NEC implementation, the PBM antennas were modelled using NEC4 [7] (which may be different than the one used in [5]). The segmentation, wire radii and coordinates for the maxima reported in [5] were used; but in several cases, coordinates were estimated from graphical data, so that they are necessarily approximate. Tables 2*a* and *b* summarise the validation results. $D_{\max}^{\text{PBM}}$ and $D_{\max}^{\text{NEC4}}$, respectively, are the maximum directivities reported by PBM and computed by NEC4.

Although NEC4 effectively replicates PBM, there are some important differences. For BM #1, NEC4's

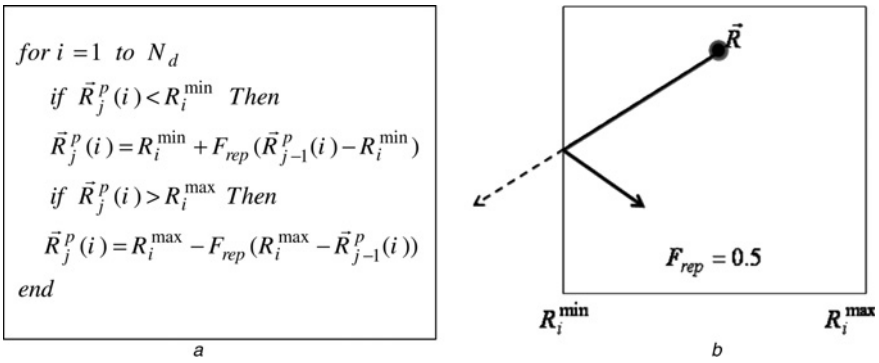

Figure 1 *Errant probe retrieval scheme*

a Errant probe reposition factor retrieval
b Illustration of probe repositioning in 2-D DS

IET Microw. Antennas Propag., 2010, Vol. 4, Iss. 5, pp. 583–592
doi: 10.1049/iet-map.2009.0147

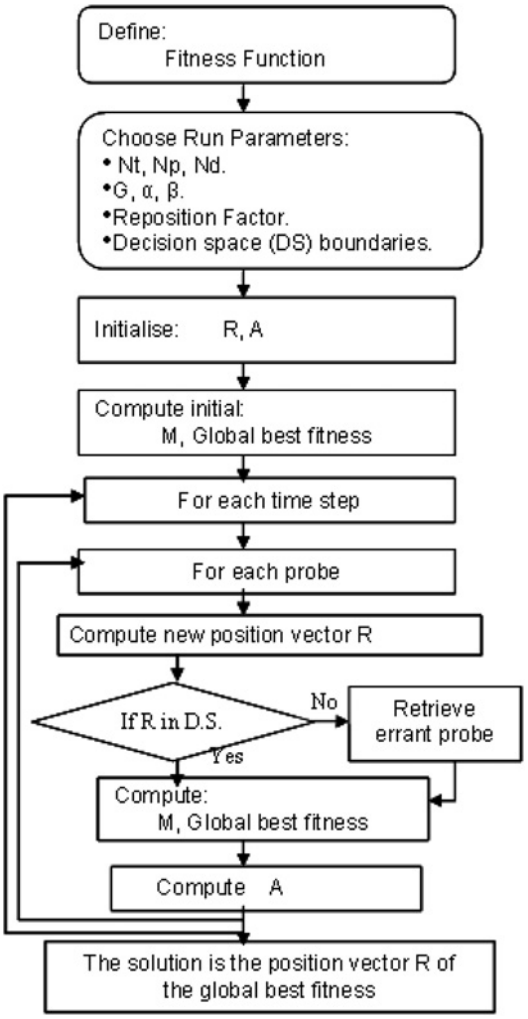

Figure 2 *Flowchart of the main steps of CFO algorithm*

computed directivity of 3.2 is slightly less than PBMs of 3.32. The same is true for BM #2, but to a lesser degree, 18.3 (PBM) against 18.11 (NEC4). For BM #3 and BM #4, the NEC4-computed directivities are lower than PBMs by a much wider margin. On BM #3, NEC4 returned a value of 6.15 compared to 7.05 from PBM. On BM #4, the NEC4 value was 4.8 compared to 5.8. The best agreement between PBM and NEC4 by far is on the last problem for which the maximum difference in directivity is only 0.1 against a value of about 19. The reasons for these

Table 2a Comparison of PBM and NEC4 results, benchmarks #1–4

BM #	PBM			NEC4
	x_1	x_2	D_{max}^{PBM}	D_{max}^{NEC4}
1	2.58λ	0.63	3.32	3.2
2	∼5.85λ[a]	$\pi/2$	∼18.3	18.11
3	0.5, 1.5, 2.5, 3.5	$\pi/2$	∼7.05	6.15
4	1.5λ	0.834	∼5.8	4.8

[a]Values marked with ∼ are estimated from Figs. 6, 9 or 11 in [5]

Table 2b Comparison of PBM and NEC4 results, benchmark #5

BM #	# Dipoles	N_d	PBM $d_i \forall i$	D_{max}^{PBM}	D_{max}^{NEC4}
5	6	5	0.99λ	∼11.25[a]	11.22
5	10	9	0.99λ	∼19	19.10
5	16	15	0.99λ	∼31	30.97
5	24	23	0.99λ	∼47	46.88

[a]Values marked with ∼ are estimated from Fig. 13 in [5]

Table 1 Properties of the PBM benchmark problems

PBM BM #	Problem characteristics	N_d	x_1	x_2	Maximise directivity
1	variable length centre fed dipole. Unimodal, single global maximum with strong local maxima	2	$0.5\lambda \le L \le 3\lambda$	$0 \le \theta \le \pi/2$	$D(L, \theta)$
2	uniform ten-element array of centre fed $\lambda/2$-dipoles. Added Gaussian noise, single global maximum with multiple strong local maxima	2	$5\lambda \le d \le 15\lambda$	$0 \le \theta \le \pi$	$D(d, \theta)$
3	eight-element circular array of centre fed $\lambda/2$-dipoles. Highly multimodal, four global maxima	2	$0 \le \beta \le 4$	$0 \le \theta \le \pi$	$D(\beta, \theta)$
4	Vee dipole. Uni-modal, single global maximum, 'smooth' landscape	2	$0.5\lambda \le L_{total} \le 1.5\lambda$	$\frac{\pi}{18} \le \alpha \le \frac{\pi}{2}$	$D(L_{total}, \alpha)$
5	Collinear N_{el}-element array of centre fed $\lambda/2$-dipoles. Uni-modal, single global maximum	$(N_{el} - 1)$	$0.5\lambda \le d_i \le 1.5\lambda$ $1 \le i \le N_{el} - 1$		$D(d_i)$

discrepancies are not clear, and there are many plausible explanations that are not discussed here.

3.3 CFO performance summary

All CFO runs were made with the following empirically determined parameters: $\alpha = 2$, $\beta = 2$, $G = 2$, with N_t and N_p varying run to run. The repositioning factor, F_{rep}, was variable following the procedure in [6]. Initial probes for BMs #1–#4 are shown in Fig. 3, while for BM #5 they were on the DS diagonal at $\boldsymbol{R}_0^p = \sum_{i=1}^{N_d} (0.5 + (p/3))\,\hat{e}_i$, $1 \le p \le N_p$ with $N_p = 2N_d$.

Effectiveness: The measure of CFO's effectiveness is how accurately it locates the PBM maxima, both coordinates and fitnesses. Table 3 provides a summary, whereas Tables 4 and 5 contain details. The fractional error in Table 3 is computed as a percentage of the PBM value which is used as the reference. For BM #1, the coordinates agree to better than 2%, while the error in directivity is somewhat higher at 3.43%. BM #2 exhibits the best agreement with a maximum error of 1.26% in the abscissa. For BM #3 the directivities differ by nearly 28%, but the results in Table 2 raise questions as to how accurate the PBM directivity is. Using the PBM coordinates for the maximum, NEC4 computes a directivity nearly 13% lower than PBMs. In this case, the abscissas disagree by about 4%, which may be a result of error in the visual estimation.

For BM #4, CFO and PBM are in very good agreement on the abscissa and directivity, but not the ordinate for which the error is nearly 15%. As with BM #3, this result alone might be troubling. The data in Table 2, however, suggest that the PBM ordinate may be incorrect, which

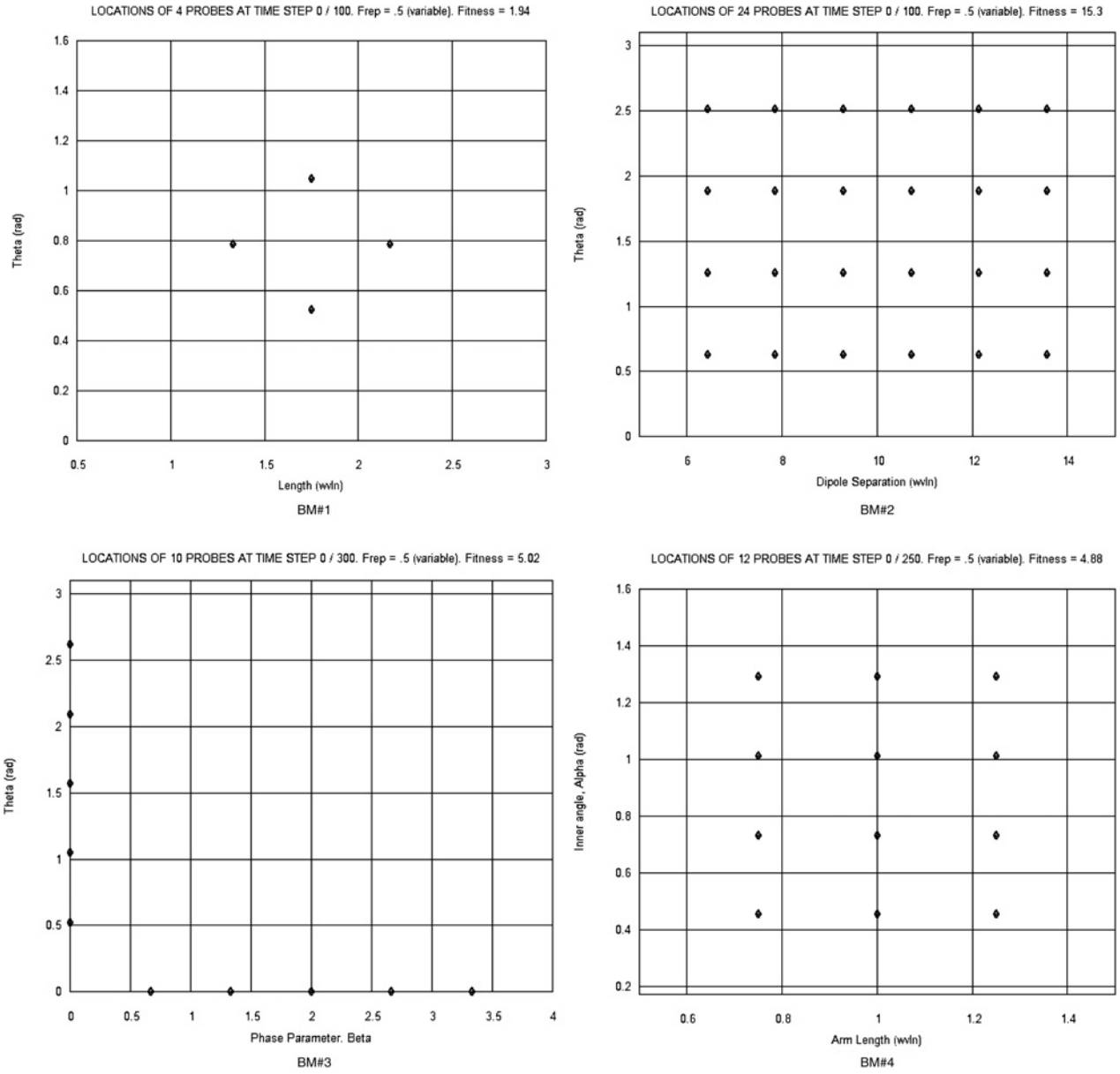

Figure 3 *Initial probes for 2D benchmarks #1–4*

doi: 10.1049/iet-map.2009.0147

Table 3 CFO effectiveness (% difference, CFO-PBM)

PBM BM #	|Δ| (%)		
	x_1	x_2	D_{max}
1	1.12	1.9	3.43
2a (without noise)	1.26	0.89	0.36
2b (with noise)	nr[a]	nr	nr
3	3.95	0.16	27.74
4	0.03	14.75	1.47
–	$d_i, i = 1, \ldots, N_{el} - 1$		—
5 (6 el)	0.11		0.26
5 (7 el)	0.70		nr
5 (10 el)	0.43		0.52
5 (13 el)	0.64		nr
5 (16 el)	0.04		0.08
5 (24 el)	1.01		0.25

[a]nr – not reported in [5]

would account for the disagreement. Using PBM's coordinates, the NEC4 validation returned a directivity of 4.8 compared to PBM's value of 5.8. This discrepancy is significant because NEC's directivity values are generally in good agreement with PBMs when the same coordinates are used. An error in the PBM ordinate also is suggested by the fact that CFO's directivity agrees with PBMs to within less than 1.5%, but only at the substantially different ordinate. For BM #5, the agreement between CFO and PBM is very good. The array element centre-to-centre spacings d_i, all of which should be 0.99λ, differ at most by 1.01%. The directivities agree to within 0.52% or better across all array sizes.

Coordinate data appear in Table 4. As pointed out above, substantial differences between PBM and CFO appear in the abscissas for BM #3 and the ordinates for BM #4. For BM #3, the global maximum's location at $\beta = 0.5$, $\theta = \pi/2$ is known analytically. But because no computed value was reported in [5], the true degree of agreement cannot be known. For BM #4, the discrepancy in the inner angle α may be a result of modelling differences, or possibly the use of different versions of NEC. All the other data in Table 4 show very good agreement.

Table 5 compares the difference of PBMs and CFO's computed directivities (fitnesses), $D_{max}^{PBM} - D_{max}^{CFO}$. The agreement is very good in all cases except BM #3. NEC4 returned a directivity 6.15 at $(\beta, \theta) = (i - 0.5, \pi/2)$, $i = 1, \ldots, 4$, instead of 7.05 as reported in [5]. If, in fact, 6.15 is the correct value, which appears to be the case, then the difference decreases to a more modest 5.47%. It seems reasonable to conclude that CFO did accurately locate the first global maximum for BM #3 after all. On BM #5 the directivity values are in excellent agreement across all array sizes.

The reasonable conclusion drawn from these data is that CFO accurately recovered the global maxima across the entire PBM benchmark suite, with the caveat that only one of the four maxima for BM #3 was located. By comparison, CFO performed better than the four algorithms described in [5]. No algorithm was 100% effective, so that CFO's effectiveness is noteworthy in view of its inchoate status as an optimisation metaheuristic.

Efficiency: The measure of an EA's efficiency is the total number of calculations required to locate global maxima, typically marked by saturation of the best fitness. This metric was applied to four algorithms in [5]: GA-FPC, μGA, GA-RC, and PSO. As their names imply, the first three are genetic algorithm variants, and the fourth is a particle swarm. Table 6 compares CFO's efficiency against the results in [5] (best values in bold italics and second best in italics).

Table 4 Comparison of PBM and CFO coordinates for maxima

PBM BM #	PBM coordinates		CFO coordinates		Δ	
	x_1	x_2	x_1	x_2	$x_1^{PBM} - x_1^{CFO}$	$x_2^{PBM} - x_2^{CFO}$
1	2.58λ	0.63	2.55088λ	0.61805	0.02912λ	0.01195
2a (no noise)	$\sim 5.85\lambda$	$\pi/2$	5.92359λ	1.55685	-0.07359λ	0.01395
2b (noise)	nr[a]	nr	6.93601λ	1.54721	–	–
3	0.5	$\pi/2$	0.48024	1.57327	0.01976	−0.00247
4	1.5λ	0.834	1.49520λ	0.71098	0.00048λ	0.12302
–	$d_i, i = 1, \ldots, N_{el} - 1$		$d_i, i = 1, \ldots, N_{el} - 1$		$\text{MAX}(d_i^{PBM} - d_i^{CFO})$	
5	0.99λ		$0.98310\lambda - 1\lambda$		0.01λ	

[a]Not reported in [5]

Table 5 Comparison of PBM and CFO best fitnesses

PBM BM #	CFO results			D_{max}^{PBM}	$\Delta D_{max}^{PBM} - D_{max}^{CFO}$
	x_1	x_2	D_{max}^{CFO}		
1	2.55088λ	0.61805	3.20627	3.32	0.11373
2a (without noise)	5.92359λ	1.55685	18.3654	18.3[a]	−0.0654
2b (with noise)	6.93601λ	1.54721	18.6880	nr[b]	nr
3	0.48024	1.57327	6.48634	7.05[a]	0.56366
4	1.49520λ	0.71098	5.71479	5.8[b]	0.08521
–	$d_i, i = 1, \ldots, N_{el} - 1$		–	–	–
5 (6 el)	0.99105λ		11.2202	∼11.25[c]	0.0298
5 (7 el)	0.98310λ		13.1826	nr	–
5 (10 el)	0.99421λ		19.0985	∼19[b]	−0.0985
5 (13 el)	0.99629λ		25.0611	nr	–
5 (16 el)	0.98958λ		30.9742	∼31[b]	0.0258
5 (24 el)	1.00000λ		46.8813	∼47[b]	0.1187

[a]Values marked with are estimated from the figures in [5]
[b]nr – not reported in [5]
[c]Values marked with ∼ are estimated from Fig. 13 in [5]

On BM #1 CFO performed much better than all the others, requiring only 60 calculations compared to 1530 for PSO, the next best. On BM #2 CFO did not perform as well as GA-FPC and μGA, with and without noise, by a factor of about 2–3. Its performance was comparable to GA-RCs, and CFO did quite a bit better than PSO. On BM #3, PSO was about 17% better than CFO, but CFO out-performed the others. For BM #4, two different CFO initial probe distributions were used with the result that its performance was comparable to GA-FPCs, and quite a bit better than **μ**GAs and GA-RCs, by at least a factor of 2. However, PSO performed better than CFO by a factor of about 3. In [5, Table 2] BM #5a and 5b are 7 and 13 element collinear arrays, respectively. For BM #5a and 5b, respectively, CFO was nearly 15 and 12 times more efficient than the next most efficient algorithm, PSO.

Table 6 CFO efficiency (# function evaluations)

PBM BM #	CFO N_{eval}	Results from PBM paper [5], Table 2 (mean hit time × population)			
		GA-FPC	μGA	GA-RC	PSO
1	***60***	3140	5065	8920	*1530*
2a (no noise)	1320	***360***	*450*	1400	2280
2b (with noise)	768				
3	*1050*	1940	1685	5040	***900***
4	1488[a]	1300	3125	3800	***330***
	1155				
5a	***72***	1220	1700	nr[b]	*1050*
5b	***144***	3480	5695	nr	*1770*

[a]Different initial probe distributions
[b]Not reported in [5]

In terms of computational efficiency, CFO performs quite well in comparison to the EAs studied in [5]. CFO turned in the best performance on three benchmarks, and it was better by a wide margin. CFO turned in the second best result on

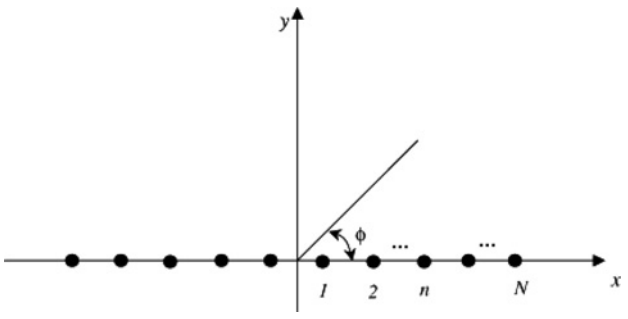

Figure 4 *Geometry of a uniform linear antenna array with 2N isotropic radiating elements* [9]

doi: 10.1049/iet-map.2009.0147

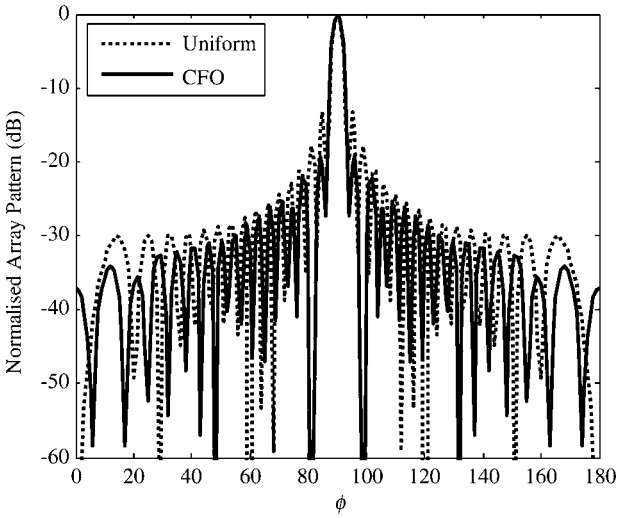

Figure 5 *Normalised radiation pattern for 32-element symmetric linear array*

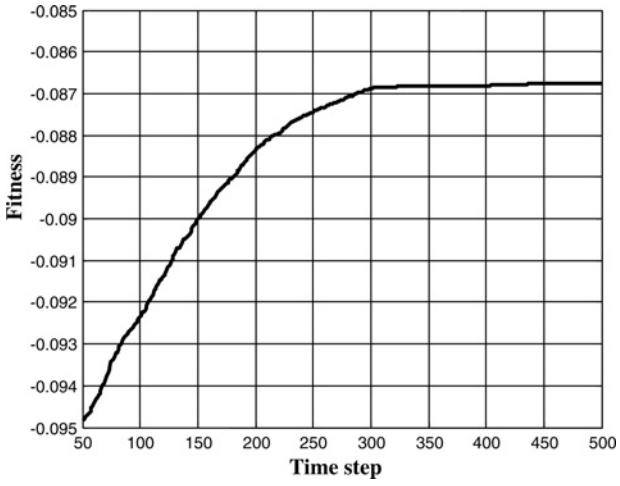

Figure 6 *Fitness against time step convergence*

BM #3, and it was close to the best efficiency. On BM #4, CFO did second best. And on BM #2 it was the third most efficient. Across all benchmarks, CFO was best on three and second best on two. PSO performed next best overall, being first on two problems and second on three. On the one BM where CFO did not finish in the top two, it was the third best. Even in its infancy, CFO's computational efficiency thus is quite competitive.

4 Linear array antenna

In [1], CFO was applied in the synthesis of a 32 (isotropic)-element linear array with null controlling, and CFO's results were compared with ACOs in [4]. In this paper, CFO is applied to the same problem, but, significantly, with a different fitness function that yields better results than those in [1, 4].

4.1 Geometry and array factor

Fig. 4 shows a linear array with $2N$ isotropic radiators symmetrically positioned around the origin along the x-axis. Each element is fed in-phase with equal amplitude excitation. In this case, the array factor simplifies to [8]

$$\mathrm{AF}(\phi) = 2\sum_{i=1}^{N} \cos(kx_i \cos(\phi)) \tag{3}$$

Table 7 Comparison among three optimisation methods for the 32-element linear array

Item	Uniform	QPM	PSO	CFO
Max. SLL (dB)	−13.29	−17.85	−19.05	−19.32
null level (dB)	−17.82	−34.74	−62.12	−83.49
fitness	−33.9	−0.789	−0.0975	−0.0867

where $k = 2\pi/\lambda$ and x_i, $i = 1, \ldots, N$ are the (dimensional) element coordinates. Here, we only optimise the positions of the array elements, x_i, to meet specific design goals for the array's pattern. Thus, in CFO we have $N_\mathrm{d} = N$.

4.2 Problem statement

The specific objective is to achieve deep nulls in prescribed directions, and minimise the sidelobe level (SLL) in the spatial regions away from the main lobe. In the context of CFO, the problem may be stated as follows: determine the coordinates of each array element x_i, $i = 1, \ldots, N$, so as to maximise a user-defined fitness function

$$\mathrm{Fitness} = -\left(\sum_i \int_{\phi_{li}}^{\phi_{ui}} \frac{|\mathrm{AF}(\phi)|^2}{\Delta\phi_i}\,\mathrm{d}\phi + \sum_k |\mathrm{AF}(\phi_{\mathrm{nu}k})|^2\right) \tag{4}$$

where the spatial regions are $[\phi_{l_1}, \phi_{u_1}] = [0^\circ, 87^\circ]$ and $[\phi_{l_2}, \phi_{u_2}] = [93^\circ, 180^\circ]$, $\Delta\phi_i = \phi_{l_i} - \phi_{u_i}$ and the null directions are $\phi_{\mathrm{nu}1} = 81^\circ$, $\phi_{\mathrm{nu}2} = 99^\circ$. CFO optimised the 32-element linear array using 1° pattern resolution with the following run parameters: $N_t = 500$, $N_p = 48$, $G = 2$, $\alpha = 0.3$ and $\beta = 1$ with negative fitness to be maximised. Unlike previously described CFO runs, a random initial probe distribution is used here according to $\vec{R}_1^p(i) = \mathbf{RU}(i) + 0.5r_1(-1^{U(r_2-0.5)})$, where RU is the uniformly spaced reference array vector $\mathbf{RU} = (\lambda/2)[0.5, 1.5, 2.5, \ldots, 15.5]$, and r_1 and r_2 are uniform random numbers between [0, 1]. The repositioning scheme for errant probe retrieval is also random as follows

$$\begin{aligned}
&\text{if } \boldsymbol{R}_j^p(i) < \mathbf{RU}(i) - 0.5(\lambda/2) \quad \text{then}\\
&\quad \boldsymbol{R}_j^p(i) = \mathbf{RU}(i) - \mathrm{random}(\lambda/2)\\
&\text{if } \boldsymbol{R}_j^p(i) > \mathbf{RU}(i) + 0.5(\lambda/2) \quad \text{then}\\
&\quad \boldsymbol{R}_j^p(i) = \mathbf{RU}(i) + \mathrm{random}(\lambda/2)
\end{aligned}$$

Table 8 Geometry of the 32-element linear array ($E_{16+i} = -E_i$), $i = 1, \ldots, 16$, obtained using four different methods

	E_i, $i = 1, \ldots, 16$
uniform	0.50, 1.50, 2.50, 3.50, 4.50, 5.50, 6.50, 7.50, 8.50, 9.50, 10.5, 11.50, 12.50, 13.50, 14.50, 15.50
QPM	0.49, 1.45, 2.35, 3.19, 3.96, 4.67, 5.37, 6.11, 6.92, 7.85, 8.89, 10.06, 11.33, 12.65, 14.01, 15.35
PSO	0.53, 1.37, 2.35, 3.11, 3.97, 4.66, 5.33, 6.11, 6.86, 7.80, 8.76, 9.900, 11.10, 12.48, 14.10, 15.51
CFO	0.56, 1.27, 2.34, 3.00, 3.92, 4.68, 5.39, 6.32, 6.97, 7.97, 8.80, 9.900, 11.04, 12.53, 14.23, 15.75

The numbers are normalised with respect to $\lambda/2$

where random(•) is a uniform random number between [0, 0.5]. The probes are restricted such that no two adjacent elements have a separation distance less than $\lambda/8$ and no element is positioned beyond $(N - 0.25)\lambda/2$ or closer than $\lambda/8$ to the origin of the x-axis. Although CFO is an inherently deterministic algorithm, the user is free to inject some measure of randomness if the performance is improved. This example is an illustration of the beneficial effects of adding a stochastic component to CFO.

4.3 Results

Fig. 5 compares the radiation patterns for the CFO-optimised 32-element linear array (solid) and a uniform array with $\lambda/2$ spacing (dotted). Table 7 lists key performance measures for CFO and two other optimisation methods: PSO [9] and QPM (quadrature programming method) [10]. CFO met the null objective of -83 dB while maintaining a maximum SLL of -19.32 dB (an improvement of 6 dB over the uniform array antenna). By comparison, the maximum SLL in [1] was -14.84 dB, so that the CFO implementation reported here achieved a substantially better result. The fitness evolution is plotted in Fig. 6. The best fitness increased monotonically through about step 300, thereafter plateauing with slight increases through about step 435. Table 7 shows that CFO's performance is slightly better than PSOs, and both PSO and CFO are considerably better than QPM. The array element coordinates appear in Table 8. None of the EAs produced a 'surprise' design in the sense that all the coordinates are close in value.

5 CFO with new selection scheme

CFO's attractive features include its simplicity, efficiency and its ability to find multiple global optima when the run parameters (N_t, N_p, F_{rep}, G, α and β) are chosen carefully. However, CFO may become trapped at local optima, especially in complex optimisation problems, and all the more so because it is deterministic. This paper introduces a new, simple 'selection scheme' to mitigate trapping as follows

$$\text{if} \quad M_j^p < M_{j-1}^p \quad \text{then} \quad \boldsymbol{R}_j^p = \text{rand}\,(\boldsymbol{R}_j^p + \boldsymbol{R}_{j-1}^p)$$

where rand is a uniform random number on [0, 1]. This approach does not guaranty that probes will not fly outside the DS. But numerical experiments using an 'invisible wall' show that the combination of the errant probe retrieval scheme and this new selection scheme is very effective in mitigating local trapping.

6 Circular array antenna

CFO with new selection scheme is applied here to optimise a ten-element circular array. The results are compared to those obtained using GA [11] and PSO [12].

6.1 Geometry and array factor

We consider a ten (isotropic)-element, non-uniform circular antenna array of radius a lying in the xy-plane, as shown in Fig. 7. In the xy-plane, the array factor for this circular array is given by [8]

$$\text{AF}(\phi) = \sum_{n=1}^{N} I_n \exp(\text{j}(ka\cos(\phi - \phi_n) + \alpha_n)) \qquad (5)$$

where $N = 10$. The aperture is $ka = (2\pi/\lambda)a = \sum_{i=1}^{N} d_i$, and the angular position of the nth element in the xy-plane is $\phi_n = (2\pi/ka)\sum_{i=1}^{n} d_i$. The nth element excitation amplitude and phase are I_n and α_n, respectively. The arc length from element n to element $n - 1$ normalised to λ is

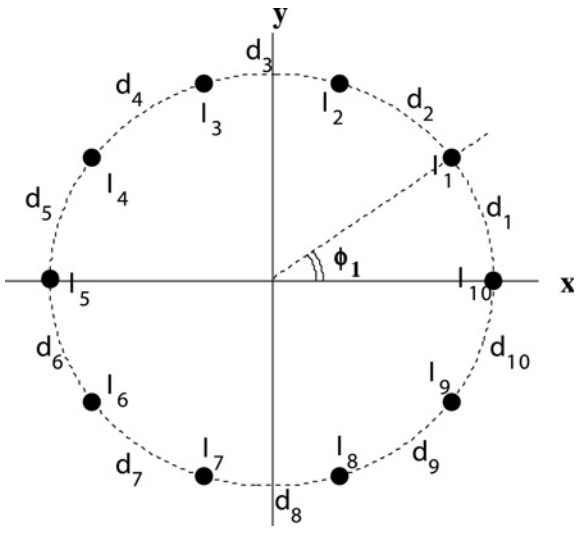

Figure 7 *Geometry of a non-uniform circular antenna array with ten isotropic radiators*

doi: 10.1049/iet-map.2009.0147

d_n, d_1 being the arc length between elements 1 and 2 as shown. The excitation phase can be adjusted to place the main lobe in the direction ϕ_0, where $\alpha_n = -ka\cos(\phi_0 - \phi_n)$. Setting $\phi_0 = 0^\circ$ for convenience, the array factor simplifies to

$$\mathrm{AF}(\phi) = \sum_{n=1}^{N} I_n \exp(\mathrm{j}ka(\cos(\phi - \phi_n) - \cos(\phi_n))) \quad (6)$$

6.2 Problem statement

The design objectives are: minimum sidelobes, and deep nulls at $\phi_{\mathrm{nu}\,1} = -27.925^\circ$ and $\phi_{\mathrm{nu}\,2} = 27.925^\circ$ (first null beamwidth FNBW $= \phi_{\mathrm{nu}\,2} - \phi_{\mathrm{nu}\,1} = 55.85^\circ$). In the context of CFO, the problem is: determine d_i, $0.25 < d_i < 1.65$, $i = 1, \ldots, N$, and I_i, $0.3 < I_i \leq 1$, $i = 1, \ldots, N$, where $N_\mathrm{d} = 2N$, so as to maximise the user-defined fitness function

$$\mathrm{Fitness} = -(0.25(0.75^{U(-130-\mathrm{sum(RPDB)})}) \times \mathrm{sum(RPDB)} + 1.5\mathrm{sum(MaxSLL)}) \quad (7)$$

where

$$\mathrm{sum(RPDB)} = \sum_k 20\log_{10}\left|\frac{\mathrm{AF}(\phi_{\mathrm{nu}\,k})}{\mathrm{AF}(0^\circ)}\right|$$

$$\mathrm{sum(MaxSLL)} = \sum_k 20\log_{10}\left|\frac{\mathrm{AF}(\phi_{\mathrm{ms}\,k})}{\mathrm{AF}(0^\circ)}\right|$$

and ϕ_{ms1}, ϕ_{ms2} are the angles at which the maximum sidelobes occur in the lower band $[-180, \phi_{\mathrm{nu1}}]$ and in the upper band $[\phi_{\mathrm{nu2}}, 180]$, respectively. The initial probe distribution is random with zero acceleration. Errant probes are retrieved using the reposition factor with $F_{\mathrm{rep}} = 0.9$, and the new selection scheme of Section 5 is used. Other run parameters are $N_t = 7500$, $N_\mathrm{p} = 20$, $G = \alpha = \beta = 2$ and $N_\mathrm{d} = 20$.

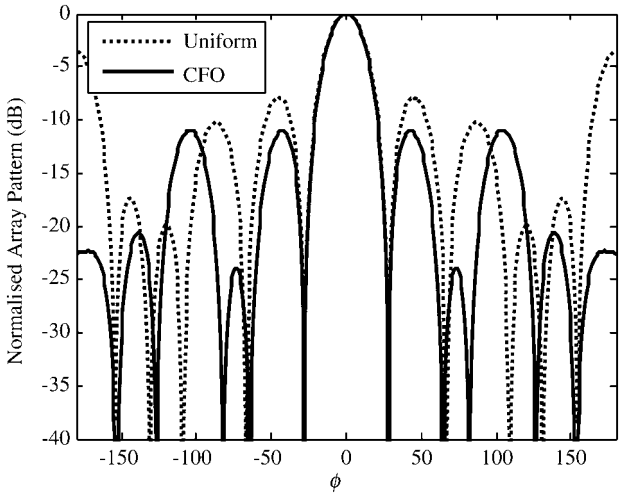

Figure 8 *Normalised radiation pattern of ten elements circular array*

Table 9 Comparison among three optimisation methods for the designed circular array

Item	Uniform	GA	PSO	CFO
Max. SLL1 (dB)	−3.6	−11.15	**−12.31**	−10.93
Max. SLL2 (dB)	−3.6	−10.85	**−12.31**	−10.93
null level1 (dB)	−47.6	−33.12	−50.38	**−64.98**
null level2 (dB)	−47.6	−27.64	−50.48	**−64.98**
aperture	**5**	6.09	5.903	5.833
fitness	34.6	48.2	62.15	**65.296**

6.3 Results

Fig. 8 compares radiation patterns of the CFO-optimised circular array (solid) and a uniform circular (dotted). Table 9 lists key performance measures for CFO and the other EAs. CFO meets the design goals by using an objective function that balances the null/SLL requirements. It achieves null levels around −65 dB and maximum SLL of about −11 dB. Fig. 9 plots CFO's best fitness evolution, which increases monotonically stepwise through about step 6350 and exhibits the typical rapid initial increase through step 1000. Thereafter, the plateaus are longer in duration, although the first three jumps in fitness are greater than those between about steps 600 and 1000. As Table 9 shows, while CFO did return the best overall fitness, its maximum SLL is 1.4 dB greater than that obtained by PSO. However, CFO produced null levels that were more than 14 dB deeper. Table 10 lists the optimised d_i and I_i values. In what might be considered a somewhat curious but very beneficial result, CFO returns a design with uniform amplitude excitation. This result is quite significant because the circular array with uniform amplitude excitation is much easier and less expensive to build than one with non-uniform amplitude and phase.

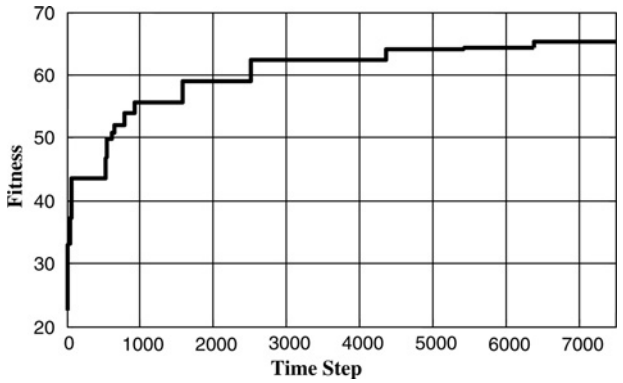

Figure 9 *Fitness against time step convergence*

Table 10 Geometry (normalised to λ) and excitation of ten-element circular array elements obtained using four different methods

uniform	d_n	0.5, 0.5, 0.5, 0.5, 0.5, 0.5, 0.5, 0.5, 0.5, 0.5
	I_n	1.0, 1.0, 1.0, 1.0, 1.0, 1.0, 1.0, 1.0, 1.0, 1.0
GA	d_n	0.3641, 0.4512, 0.2750, 1.6373, 0.6902, 0.9415, 0.4657, 0.2898, 0.6456, 0.3282
	I_n	0.9545, 0.4283, 0.3392, 0.9074, 0.8086, 0.4533, 0.5634, 0.6015, 0.7045, 0.5948
PSO	d_n	0.3170, 0.9654, 0.3859, 0.9654, 0.3185, 0.3164, 0.9657, 0.3862, 0.9650, 0.3174
	I_n	1.0, 0.7529, 0.7519, 1.0, 0.5062, 1.0, 0.7501, 0.7524, 1.0, 0.5067
CFO	d_n	0.3688, 0.7263, 0.7263, 0.7263, 0.3688, 0.3688, 0.7263, 0.7263, 0.7263, 0.3688
	I_n	0.6675, 0.6675, 0.6675, 0.6675, 0.6675, 0.6675, 0.6675, 0.6675, 0.6675, 0.6675

7 Conclusions

CFO is a new optimisation EA whose performance has been studied on the PBM antenna benchmark suite and on two-array synthesis problems. This paper also introduces a new selection scheme for mitigating trapping, and compares CFO to other EAs. Even though in its infancy, CFO exhibits robust performance and holds out what appears to be considerable promise if certain issues can be addressed. For example, at this point there is no methodology for choosing CFO run parameters, yet how well CFO works can be very sensitive to their values. CFO's deterministic nature, coupled with its frequently rapid convergence, even if to a local maximum, may help users to quickly specify suitable run parameters. These attributes also may make CFO an excellent candidate for real-time 'parameter tuning' in which run parameters are changed in response to the algorithm's behaviour. The examples reported here suggest that CFO merits consideration by engineers actively engaged in antenna design, and also by theoreticians interested in exploring and further developing new concepts in optimisation.

8 References

[1] FORMATO R.A.: 'Central force optimization: a new metaheuristic with application in applied electromagnetics', *Prog. Electromagn. Res.*, 2007, **77**, pp. 425–491

[2] FORMATO R.A.: 'Central force optimization: a new nature inspired computational framework for multidimensional search and optimization', in KRASNOGOR N., NICOSIA G., PAVONE M., PELTA D. (EDS.): 'Studies in computational intelligence (SCI)' (Springer, Heidelberg, 2008), vol. 129, pp. 221–238

[3] ROBINSON J., RAHMAT-SAMII Y.: 'Particle swarm optimization in electromagnetics', *IEEE Trans. Antennas Propag.*, 2004, **52**, (2), pp. 397–407

[4] RAJO-IGLESIAS E., QUEVEDO-TERUEL O.: 'Linear array synthesis using an ant-colony optimization-based algorithm', *IEEE Antennas Propag. Mag.*, 2007, **49**, (2), pp. 70–79

[5] PANTOJA M.F., BRETONES A.R., MARTIN R.G.: 'Benchmark antenna problems for evolutionary optimization algorithms', *IEEE Trans. Antennas Propag.*, 2007, **55**, (4), pp. 1111–1121

[6] FORMATO R.A.: 'Central force optimization: a new deterministic gradient-like optimization metaheuristic', *OPSEARCH, J. Oper. Res. Soc. India (ORSI)*, 2009, **46**, (1), pp. 25–51

[7] BURKE G.J.: 'Numerical electromagnetics code – NEC-4, method of moments, part i: user's manual and part ii: program description – theory'. UCRL-MA-109338, Lawrence Livermore National Laboratory, Livermore, California, USA, January 1992 (https://ipo.llnl.gov/technology/software/softwaretitles/nec.php)

[8] BALANIS C.A.: 'Antenna theory: analysis and design' (Wiley, New York, 1997)

[9] KHODIER M., CHRISTODOULOU C.: 'Linear array geometry synthesis with minimum sidelobe level and null control using particle swarm optimization', *IEEE Trans. Antennas Propag.*, 2005, **53**, (8), pp. 2674–2679

[10] GODARA L.C.: 'Handbook of antennas in wireless communications' (CRC, Boca Raton, FL, 2002)

[11] PANDURO M., MENDEZ A., DOMINGUEZ R., ROMERO G.: 'Design of non-uniform circular antenna arrays for side lobe reduction using the method of genetic algorithms', *Int. J. Electron. Commun. (AEU)*, 2006, **60**, pp. 713–717

[12] SHIHAB M., NAJJAR Y., DIB N., KHODIER M.: 'Design of non-uniform circular antenna arrays using particle swarm optimization', *Electr. Eng. J. (JEEEC)*, 2008, **29**, (4), pp. 216–220

doi: 10.1049/iet-map.2009.0147